Cancer Immunol Immunother (2015) 64:817–829
DOI 10.1007/s00262-015-1692-6

ORIGINAL ARTICLE

# Liver myeloid-derived suppressor cells expand in response to liver metastases in mice and inhibit the anti-tumor efficacy of anti-CEA CAR-T

**Rachel A. Burga[1,2] · Mitchell Thorn[1,2] · Gary R. Point[1,2] · Prajna Guha[1,2] · Cang T. Nguyen[1,2] · Lauren A. Licata[1,2] · Ronald P. DeMatteo[3] · Alfred Ayala[4] · N. Joseph Espat[1,2] · Richard P. Junghans[5] · Steven C. Katz[1,2]**

Received: 26 June 2014 / Accepted: 26 March 2015 / Published online: 8 April 2015


**Abstract** Chimeric antigen receptor-modified T cell (CAR-T) technology, a promising immunotherapeutic tool, has not been applied specifically to treat liver metastases (LM). While CAR-T delivery to LM can be optimized by regional intrahepatic infusion, we propose that liver CD11b+Gr-1+ myeloid-derived suppressor cells (L-MDSC) will inhibit the efficacy of CAR-T in the intrahepatic space. We studied anti-CEA CAR-T in a murine model of CEA+ LM and identified mechanisms through which L-MDSC expand and inhibit CAR-T function. We established CEA+ LM in mice and studied purified L-MDSC and responses to treatment with intrahepatic anti-CEA CAR-T infusions. L-MDSC expanded threefold in response to LM, and their expansion was dependent on GM-CSF, which was produced by tumor cells. L-MDSC utilized PD-L1 to suppress anti-tumor responses through engagement of PD-1 on CAR-T. GM-CSF, in cooperation with STAT3, promoted L-MDSC PD-L1 expression. CAR-T efficacy was rescued when mice received CAR-T in combination with MDSC depletion, GM-CSF neutralization to prevent MDSC expansion, or PD-L1 blockade. As L-MDSC suppressed anti-CEA CAR-T, infusion of anti-CEA CAR-T in tandem with agents targeting L-MDSC is a rational strategy for future clinical trials.

**Keywords** Liver metastases · CAR-T · MDSC · Immunosuppression · GM-CSF

**Abbreviations**

| | |
|---|---|
| ALL | Acute lymphoblastic leukemia |
| BM | Bone marrow |
| CAR-T | Chimeric antigen receptor-modified T cells |
| CEA | Carcinoembryonic antigen |
| CLL | Chronic lymphocytic leukemia |
| FMO | Fluorescence minus one |
| GM-CSF | Granulocyte–macrophage colony-stimulating factor |
| IDO | Indolamine 2,3-dioxygenase |
| IFNγ | Interferon gamma |
| IL2 | Interleukin 2 |
| iNOS | Inducible nitric oxide synthase |
| LM | Liver metastases |
| L-MDSC | Liver myeloid-derived suppressor cells |
| NO | Nitric oxide |
| NPC | Non-parenchymal cells |
| PD-1 | Programmed death 1 |
| PD-L1 | Programmed death ligand 1 |
| pSTAT3 | Phosphorylated signal transducer and activator of transcription 3 |
| SSG | Sodium stibogluconate |
| STAT3 | Signal transducer and activator of transcription 3 |
| UT | Unmodified/untransduced T cells |

Rachel A. Burga and Mitchell Thorn have contributed equally to this work.

✉ Steven C. Katz
skatz@chartercare.org

[1] Division of Surgical Oncology, Department of Surgery, Roger Williams Medical Center, 825 Chalkstone Avenue, Prior 4, Providence, RI 02908, USA

[2] Boston University School of Medicine, Boston, MA, USA

[3] Department of Surgery, Memorial Sloan-Kettering Cancer Center, New York, NY, USA

[4] Department of Surgery and Immunology Laboratory, Rhode Island Hospital, Warren Alpert Medical School of Brown University, Providence, RI, USA

[5] Department of Medicine, Roger Williams Medical Center, Providence, RI, USA

## Introduction

Liver metastases (LM) develop in over 50 % of patients with colorectal cancer [1]. Surgical resection of colorectal cancer LM is potentially curative in only a subset of patients [2], and modern cytotoxic chemotherapy also fails to provide definitive treatment, with response rates ranging from 33 to 51 % [3, 4]. We are interested in developing immunotherapeutic strategies for LM as alternatives to conventional approaches. Recent studies suggest that a robust host T cell response to LM is associated with prolonged survival [5, 6]. Unfortunately, most patients do not develop an effective immune response to LM and die of their disease. LM may escape immune surveillance due to the immunosuppressive nature of the intrahepatic space [6]. Suppressive immune cells within the liver may not only challenge endogenous immunity, but also impair effectiveness of immunotherapeutic treatments. As such, highly specific anti-tumor immunotherapy coupled with targeting of suppressive cells in the intrahepatic tumor environment is a rational approach for LM therapy.

Renewed optimism for anti-tumor immunotherapy has resulted from recent trials [7, 8]. Chimeric antigen receptor-modified T cells (CAR-T) have shown promise for treatment of ALL, CLL, and melanoma [9–11]. In the present study, we utilized T cells engineered to express a CAR specific for carcinoembryonic antigen (CEA), a tumor antigen expressed by colorectal cancer LM [12]. This highly specific CAR enables anti-CEA CAR-T to bypass antigen processing and presentation and mediate tumor killing in vitro and in vivo [13]. This work was conducted in parallel with a phase I trial (NCT01373047) that examined the safety and efficacy of anti-CEA CAR-T infused regionally in patients with unresectable CEA+ LM [14]. Although anti-CEA CAR-T have demonstrated efficacy in vitro and in vivo [13], immunosuppression in the liver is likely to be an important barrier to achieving optimal clinical results for patients with LM.

The intrahepatic space contains an abundance of suppressive cells including liver myeloid-derived suppressor cells (L-MDSC) [15–17]. L-MDSC are a heterogeneous population of myeloid cells at various stages of differentiation, identified in mice on the basis of a CD11b+Gr-1+ phenotype [18]. Evidence suggests that the extent of MDSC expansion is related to both tumor burden and disease stage [19]. Although we can deplete L-MDSC in mice through targeting of Gr-1 (Ly6-G/Ly6-C), this approach is not possible in patients due to the lack of a suitable marker for human MDSC. Therefore, we investigated factors driving L-MDSC expansion and suppressive function within the context of LM and CAR-T treatment, to identify translatable targets.

While MDSC are well known to inhibit conventional T cells in a variety of settings, how L-MDSC may suppress CAR-T designed to target CEA+ LM is unclear. We speculate that L-MDSC engage immunoinhibitory pathways to suppress CAR-T, as CAR-T increase programmed death-1 (PD-1, CD279) expression following infusion into solid tumor patients [20]. PD-1 engagement by its ligand, PD-L1, has been shown to impair T cell proliferation, in addition to inhibiting production of IL-2 and IFNγ [21]. The present work defines potential strategies for enhancing the efficacy of CAR-T for treatment of LM by blocking the immunoinhibitory effects of L-MDSC, providing the rationale for development of future phase I studies.

## Materials and methods

### Animals

Six- to ten-week-old male C57BL/6J mice were purchased from Jackson Laboratories (Bar Harbor, ME). Six-week-old male CEA transgenic mice (C57BL/6-*H-2*$^{b}$-*Tg(cosCEA1)2682*) were a generous gift from Dr. Jeffrey Schlom at the NIH. PD-1$^{-/-}$ mice (C57BL/6-*Pdcd1*$^{-/-}$) were a generous gift from Dr. Tasuku Honjo, Kyoto University via Dr. Alfred Ayala, Brown University School of Medicine, and were bred in-house, with 6- to 10-week-old males used for experiments. Animals were maintained in a pathogen-free environment, and experiments were conducted in compliance with the Roger Williams Medical Center Institutional Animal Care and Use Committee.

### CAR-T cell production

Spleens were harvested from C57BL/6J or PD-1$^{-/-}$ mice, red blood cells lysed (ACK Lysing Buffer, Gibco by Life Technologies, Grand Island, NY), and splenocytes isolated. Splenocytes were activated in 750-mL flasks (BD Falcon) with 1 μg/mL anti-CD3 (eBioscience), 1 μg/mL anti-CD28 (eBioscience) and 1.2 ng/mL recombinant murine IL-2 (R&D Systems, Minneapolis, MN) in RPMI with L-glutamine (Corning: Cellgro, Manassas, VA) supplemented with 10 % filtered and heat-inactivated sterile fetal bovine serum (Sigma-Aldrich, St. Louis, MO) and 1 % antibiotic/antimycotic (Corning: Cellgro, Manassas, VA). Retroviral supernatant containing genes for tandem molecules of hMN14 sFv-CD8α fused to a hybrid CD28/CD3ζ CAR was used to transduce activated splenocytes as previously described [13] over a 3- to 5-day period to create second-generation anti-CEA CAR-T. Anti-CEA CAR-T were maintained in RPMI supplemented as above with 1.2 ng/mL IL2 and were used for in vitro or in vivo experimentation immediately following assessment of transduction efficiency.

### Tumor injections

C57BL/6 mice were anesthetized with 2 % isoflurane, their spleens injected with 2.0–2.5 × $10^6$ MC38 or MC38CEA tumor cells, and, following 2 min of applied pressure, splenectomy was performed. Splenectomy alone had no significant impact on liver MDSC populations (not shown). MC38 and MC38CEA cells were a generous gift from Dr. Jeffrey Schlom. We created MC38CEA-luc cells by infection of target MC38CEA cells by pLenti-III-UbC-Luciferase (Applied Biological Materials Inc, Richmond, BC, Canada) lentivirus supernatant over an 8-h period, after which cells were further subcultured. Puromycin (0.3 μg/mL, Sigma-Aldrich) was used to select for stable cell lines, and clones with optimal luciferase expression were isolated and expanded. LM were detectable by bioluminescence as early as 2 days following splenic injection. "Normal" animals are identified as control C57BL/6 mice that had not received any surgical modifications.

### Cell isolation

Liver non-parenchymal cells (NPC) were isolated from tumor-bearing mice as previously described with modifications [16]. Briefly, following euthanization, we injected the portal vein with 3 mL 0.01 % (w/v) collagenase IV (Sigma-Aldrich) prepared in PBS and the liver extracted, mechanically disrupted, and incubated for 20 min in 10 mL 0.01 % collagenase at 37 °C. Following elimination of hepatocytes by low-speed centrifugation, samples were resuspended in 3 mL RPMI, and then, 2 mL of 40 % (w/v) OptiPrep (Sigma-Aldrich) was added for density gradient separation of NPC. NPC-containing cell suspension was incubated with 1 μg anti-FcγR III/II mAb2.4G2 (Miltenyi) per 1 × $10^6$ cells. For functional assays, L-MDSC were isolated with immunomagnetic beads (CD11b+, Miltenyi Biotech, Auburn, CA) and >70 % of CD11b+ cells were found to co-express Gr-1. L-MDSC frequency among tumor-free NPC is normally 1–5 %. L-MDSC expansion and baseline phenotype in tumor-bearing livers were demonstrated by fractionating NPC with CD45 immunomagnetic beads (Miltenyi) or analyzing bulk liver NPC prior to staining with anti-Gr-1, anti-CD11c, and anti-CD11b antibodies. About 70 % of NPC were CD45+ in tumor-bearing livers. CD11c+ cells were excluded from for certain experiments; however, this did not appreciably impact liver MDSC assessments.

For analysis of whole liver lysate, extracted livers were immersed in 1 mL/0.1 g by liver weight of protease inhibitor cocktail (Sigma-Aldrich), followed by incubation in RIPA lysis buffer (Millipore, Temecula, CA) and centrifugation. For evaluation of L-MDSC phenotypic changes, cells were treated with 20 ng/mL GM-CSF (R&D Systems, Minneapolis, MN), 1.5 μM cucurbitacin I (JSI-124, Sigma-Aldrich), or 20 μM celastrol (Cayman Chemical, Ann Arbor, Michigan) for 36 h and flow cytometry performed. Bone marrow (BM) was isolated from femurs and tibias of control as well as tumor-bearing mice, and following erythrocyte lysis, cells were cultured either alone or with MC38CEA cells, MC38CEA conditioned medium, or 20 ng/mL GM-CSF, in RPMI with 10 % FBS. After 3–4 days, flow cytometry was used to determine the frequency and phenotype of BM-derived MDSC.

### Flow cytometry and antibodies

NPC were stained with antibodies specific for CD11b (M1/70), CD11c (HL3), Gr-1: Ly6G and Ly6C (RB6-8C5), pSTAT3 (pY705), PD-1 (RMP1-30, Biolegend), PD-L1 (10F.9G2, Biolegend), PD-L2 (TY25), and IL4Rα (I015F8, Biolegend). Antibodies were conjugated to FITC, PE, PerCP, APC, APC-Cy7, Pe-Cy7, or Pacific Blue (BD Biosciences unless otherwise identified) and were analyzed on the CyAn flow cytometer (Beckman Coulter). We measured CAR expression 2–3 days post-transduction by flow cytometry using the Wi2 anti-idiotype antibody for the humanized anti-CEA CAR (a generous gift from Dr. Hansen, Immunomedics, Morris Plains, NJ) conjugated to APC. CAR-T phenotype was assessed by staining with antibodies against CD3 (145-2C11), CD4 (Gk1.5), CD8 (53–6.7), and PD-1 (CD279, RMP1-30, Biolegend) conjugated to FITC, PE, PerCP, APC, APC-Cy7, or PE-Cy7 (BD Biosciences). Antibodies to phospho-STAT3 (Y705) and GAPDH-HRP monoclonal antibody were from Cell signaling. Anti-STAT3 (H-190) was purchased from Santa Cruz. Voltages were set based on unstained cells, and compensation calculated using single-stained controls. Positive staining was defined with fluorescence minus one (FMO) controls, and results were analyzed using Flow Jo 7.6.5 (Tree Star Inc., Ashland, OR). We have identified similar viability of L-MDSC when gated with live scatter gating as compared to vital dye staining and as such have presented our results from a live leukocyte scatter gating profile.

### In vitro suppression assays

CAR-T were labeled with 1 μM carboxyfluorescein diacetate succinimidyl ester (CFSE, Invitrogen, Carlsbad, CA) according to the manufacturer's protocol and were added at a 5:1 ratio with L-MDSC from tumor-bearing livers. CEA+ tumor cells were irradiated with 5000 rad and added to the culture at a 1:2 ratio with CAR-T to stimulate proliferation. The effect of in vitro blockade of PD-1 and PD-L1 signaling was examined by adding 5 μg/mL anti-PD-1 (29F.1A12, Biolegend), 5 μg/mL anti-PD-L1 (MIH5, eBioscience), or 10 μg/mL sodium stibogluconate (SSG, EMD

Millipore, Billerica, MA) to the culture. After 2–4 days, CAR-T were analyzed for CFSE dilution. Proliferation represents the percentage of cells with diluted CFSE, in reference to the undivided CFSE peak and an unstimulated cell sample (negative control).

### Western blot analysis

Cells were washed twice with ice-cold PBS and lysed with RIPA buffer (Life Technologies, Carlsbad, CA) supplemented with protease inhibitor cocktail (Roche Diagnostics, Indianapolis, IN), 1 mM NaVO4, and 1 mM NaF as described previously [22]. Lysates were centrifuged at 10,000 rpm for 10 min at 4 °C, and supernatants were collected and protein quantification was performed using Bradford protein assay (Thermo Scientific, Tewksbury, MA) with BSA as the standard. Lysates were denatured using β-mercaptoethanol (Life Technologies) and Laemmli sample buffer (Bio-Rad, Waltham, MA), heated at 70 °C for 10 min, electrophoresed in Mini Protean TGX 4–15 % gels (Bio-Rad), transferred on Trans Blot Turbo PVDF membrane (Bio-Rad), and immunoblotted with specific primary antibodies. Primary antibody binding was detected using HRP-conjugated secondary antibodies (Santa Cruz, Dallas, TX) and ECL Prime Western blot reagents (Amersham/GE Healthcare, Pittsburgh, PA) as chemiluminescence substrates. The immunoblots were analyzed and quantified using ImageJ software.

### In vivo studies

Following establishment of LM, C57BL/6 mice were treated with CAR-T or unmodified T cells (UT), at a 1:1 ratio to the amount of MC38CEA injected previously, administered directly into the portal vein. T cell treatments were administered 3 and/or 7 days following tumor establishment. Designated mice received intraperitoneal injections of 10 μg anti-Gr-1 (RB6-8C5, BD Biosciences), 10 μg anti-GM-CSF (22E9, BD Biosciences), 10 μg anti-PD-L1 (MIH5, eBioscience), or isotype control on days 2, 4, 6, 8, 10, 12, 14, and 16 post-tumor injection. All mice were injected with 0.3 μg IL2 i.p. daily following CAR-T or UT infusions. In order to quantify tumor cell killing following animal killing, flow cytometry was used to measure the percent of CD66e+ (CEA+) cells among viable liver cells (B1.1/CD66, BD Biosciences). For mice injected with MC38CEA-luc cells, 30 μg potassium luciferin (Gold Biotechnology, St. Louis, MO) was injected 15 min prior to imaging with the IVIS Lumina 100 (PerkinElmer) and total bioluminescence by photon counts (flux = photons/s) generated. Bioluminescent images were captures at 60 s exposure, with small binning and f-stop 2. We measured GM-CSF, STAT3, and pSTAT3 in tumor cell culture supernatant, whole liver lysate, and serum by ELISA (GMCSF-Thermo Scientific, Rockford, IL, STAT3/pSTAT3-eBioscience). The animals were assessed by IVIS just prior to and at the time of necroscopy to determine whether the cause was due to tumor or postoperative complications.

### Statistics

We performed statistical analysis with Prism V5.00 for Windows (GraphPad software, San Diego, CA). Statistical significance was determined using the two-tailed Student's *t* test or log-rank (Mantel–Cox) test for Kaplan–Meier generated survival data, and values with $p < 0.05$ were deemed statistically significant ($*p \leq 0.05$, $**p \leq 0.01$, $***p \leq 0.001$).

## Results

### L-MDSC expand in response to metastases and suppress anti-CEA CAR-T

We examined LM growth in C57BL/6 and C57BL/6 CEA transgenic animals and determined no significant difference in tumor development (not shown). As such, all subsequent in vivo experiments were conducted in C57BL/6 mice. Following 2 weeks of tumor growth, we demonstrated that L-MDSC expanded threefold or greater in response to LM. This expansion was CEA-independent, as it occurred equally in mice with CEA+ or CEA− LM (Fig. 1a). We confirmed that the majority of CD11b+ liver NPC co-expressed Gr-1, consistent with the MDSC phenotype (Fig. 1b). When co-cultured with CAR-T stimulated by MC38CEA cells, L-MDSC suppressed CAR-T proliferation. Division of CAR-T in response to CEA+ tumor was reduced twofold with the addition of L-MDSC (Fig. 1c).

### L-MDSC depletion improves regional CAR-T efficacy for the treatment of LM

We speculated that CAR-T efficacy in vivo would be limited by the significant L-MDSC expansion in response to LM as demonstrated above. To determine whether anti-CEA CAR-T could be protected from intrahepatic suppression by elimination of L-MDSC, we depleted Gr-1+ cells. We treated mice with anti-Gr-1 antibody on days 7 and 11 following tumor cell injection and then harvested liver tissue following 2 weeks of tumor growth to measure MDSC frequencies. Anti-Gr-1 treatment reduced the L-MDSC population to levels seen in mice without tumor, demonstrating effective depletion (Fig. 2a, b). In a subsequent study, mice with established LM were treated with CAR-T, and some groups also received anti-Gr-1. We

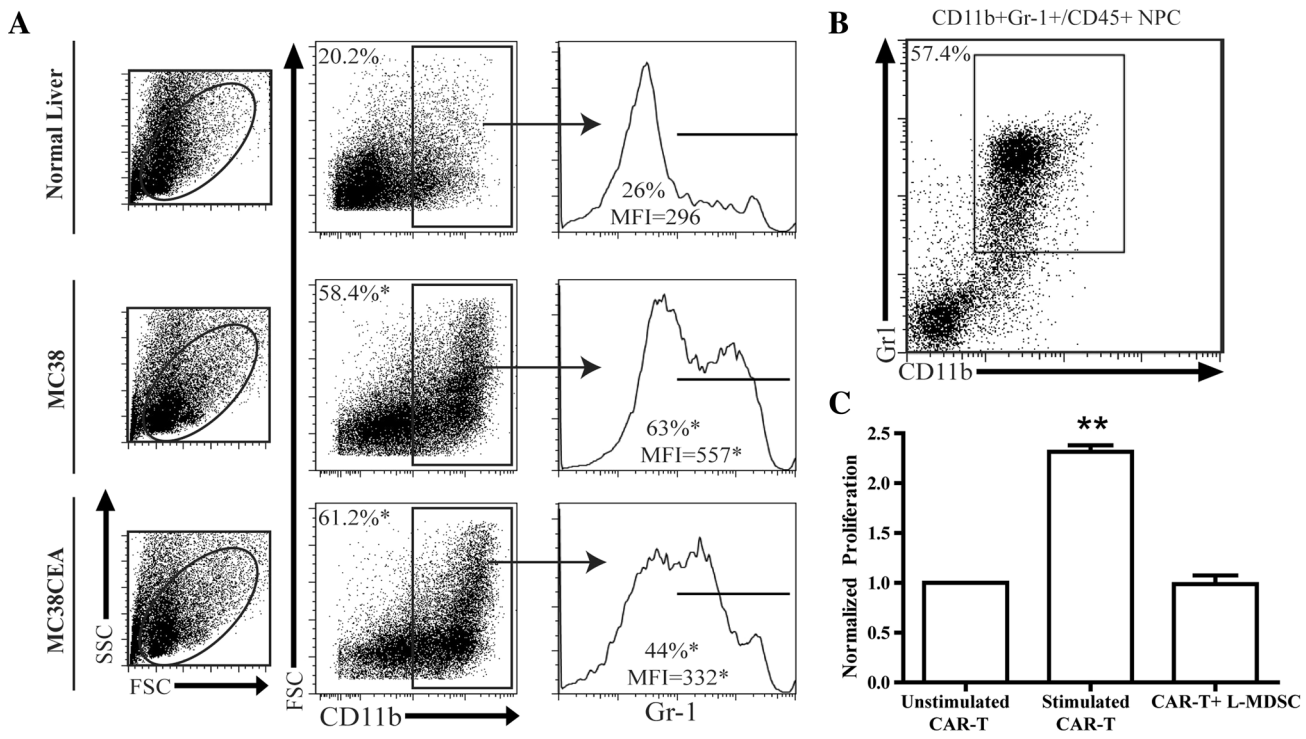


**Fig. 1** L-MDSC expand in response to LM and suppress CAR-T. LM were established by splenic injections of either MC38 or MC38CEA tumor cells, and livers were harvested 2 weeks of tumor growth. Flow cytometry was used to evaluate the expansion of L-MDSC in response to LM. **a** Sequential gating of L-MDSC as live, CD11b+, and Gr-1+ liver leukocytes from normal or tumor-bearing livers. Cells were enriched by immunomagnetic beading for CD45+ NPC prior to staining. **b** *Dot plot* confirming high level of Gr-1 and CD11b co-expression among liver leukocytes. **c** L-MDSC were co-cultured with CFSE-labeled anti-CEA CAR-T stimulated by irradiated MC38CEA cells, and pooled results from three independent experiments are graphed. The percentages of cells having undergone division (CFSE-low) were normalized to the unstimulated group. *Bar* graphs represent mean ± SEM; *dot plots* and *histograms* are representative of ≥3 mice per group and have been confirmed with at least two separate experiments (*$p \leq 0.05$, **$p \leq 0.01$)

confirmed that portal vein delivery improved anti-tumor efficacy compared to systemic infusion via tail vein, and therefore, all in vivo CAR-T were administered regionally (data not shown). L-MDSC depletion alone significantly reduced viable LM cells after 2 weeks (19.0 % UT vs. 3.3 % UT+aGr-1, Fig. 2c). The combination of anti-CEA CAR-T with L-MDSC depletion was more effective than either treatment alone (0.9 % CAR-T+aGr-1 vs. 3.3 % UT+aGr-1 vs. 5.6 % CAR-T, Fig. 2c). Additionally, anti-CEA CAR-T treatment in conjunction with L-MDSC depletion resulted in significantly prolonged survival compared to UT (Fig. 2d).

## GM-CSF drives myeloid-derived suppressor cell expansion in response to LM

As L-MDSC depletion with anti-Gr-1 is not a viable clinical strategy, we studied GM-CSF neutralization as an alternative approach. Tumor cells have been found to secrete high levels of GM-CSF in vivo, a cytokine implicated in MDSC recruitment [23–25]. By treating animals with anti-GM-CSF on days 4, 6, and 8 post-LM establishment, we found that L-MDSC expansion was significantly reduced, returning to baseline frequency (Fig. 3a). We compared L-MDSC suppressive function from LM mice treated with anti-GM-CSF and isotype control and found no significant difference (not shown). Ex vivo, liver NPC and MC38CEA tumors cells produced GM-CSF, with significantly more GM-CSF produced by tumor (10.2 pg/mL NPC vs. 36.9 pg/mL MC38CEA, $p < 0.05$). In an analysis of non-tumor (CTRL) and LM mice sacrificed at various time points following LM establishment, the kinetics of L-MDSC expansion over time were paralleled by increases in serum (Fig. 3b) and liver GM-CSF levels (Fig. 3c). Furthermore, to confirm the dependency of MDSC expansion on tumor-associated GM-CSF, we exposed BM cells to various sources of GM-CSF ex vivo. Among CD45+ BM cells, the MDSC population (CD11b+Gr-1+) was significantly increased from baseline following co-culture with tumor cells, GM-CSF, or tumor-conditioned media (Fig. 3d). We also confirmed that L-MDSC expressed the GM-CSF receptor (48.3 % GM-CSFR+, data not shown).

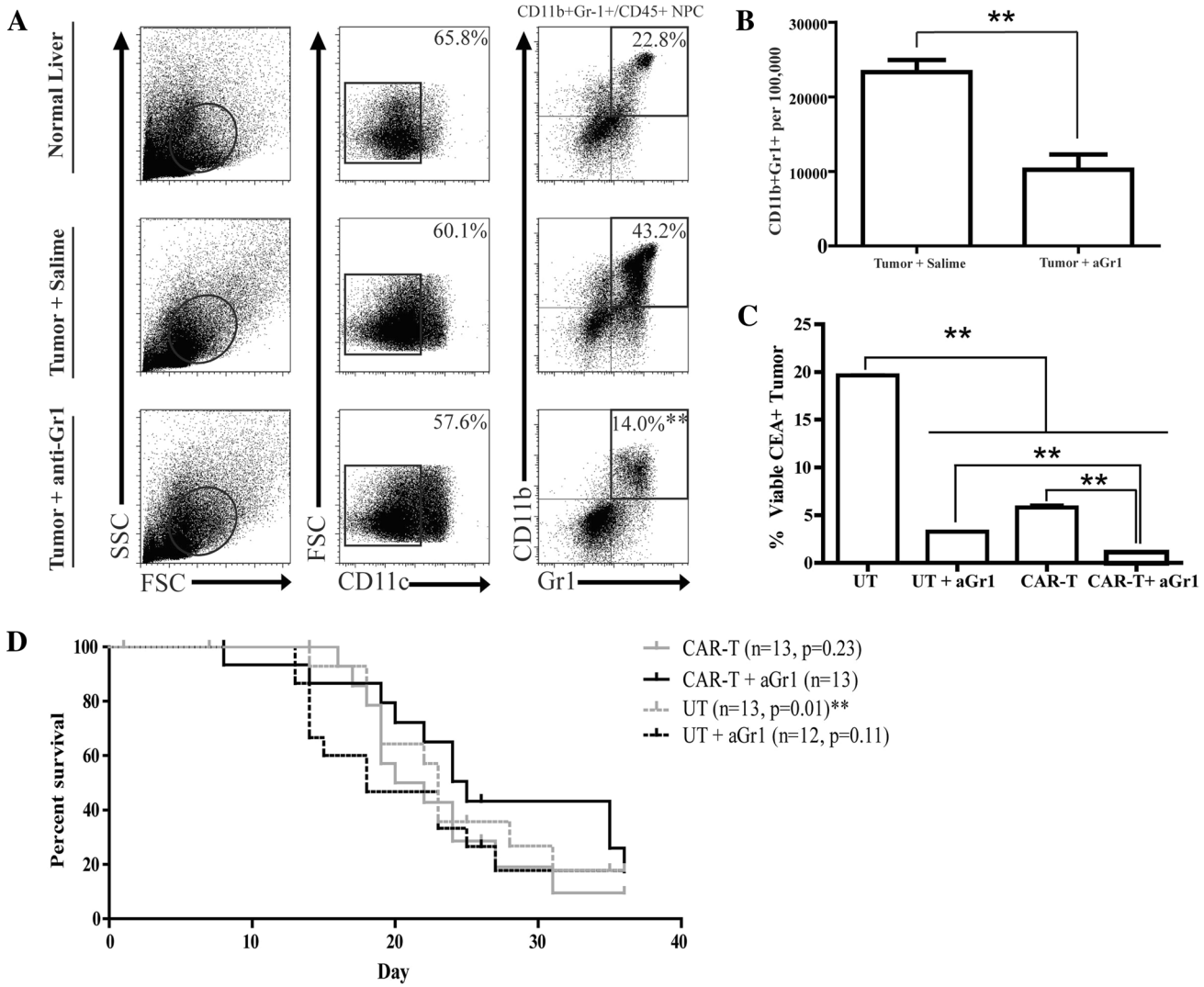


**Fig. 2** L-MDSC depletion improves CAR-T efficacy. LM were established by splenic injections of MC38CEA cells, and saline or anti-Gr-1 antibody was injected intraperitoneally on days 7 and 11 post-tumor establishment. Livers were harvested for NPC isolation, staining, and analysis after 14 days. **a** Flow cytometry *dot plots* of the L-MDSC (live, CD11c−CD11b+Gr-1+) population with or without anti-Gr-1 treatment. Cells were enriched by immunomagnetic beading for CD45+ NPC prior to staining. **b** Absolute L-MDSC numbers per 100,000 cells in liver isolate were calculated according to cell counts. **c** Mice with established LM received infusions of UT or CAR-T after 7 days, in addition to anti-Gr-1 (aGr-1) treatment in designated groups on days 7 and 11. Flow cytometry was used to determine the percentages of viable CEA+ tumor cells among all liver NPC after killing at day 26. **d** Survival curves for in vivo examination of ≥12 animals with LM treated with UT or CAR-T with and without Gr-1-antibody. *Bar graphs* represent mean ± SEM; *dot plots* are representative samples, survival significance displayed as relative to CAR-T+aGr-1 group (**$p \leq 0.01$)

## L-MDSC suppressive capabilities through the PD-1/PD-L1 axis are modulated by GM-CSF

As interaction of PD-L1 with PD-1 is a mechanism by which MDSC suppress endogenous T cells, we determined whether L-MDSC inhibit CAR-T in similar fashion. Anti-CEA CAR-T expressed PD-1 (Fig. 4a) and L-MDSC from mice with LM were found to express high levels of PD-L1 (Fig. 4b). Expression of PD-L2 by L-MDSC and PD-L1 by MC38CEA cells was negligible (data not shown). Having demonstrated that GM-CSF promoted L-MDSC expansion, we asked whether GM-CSF concurrently promoted L-MDSC PD-L1 expression. BM-derived MDSC exhibited significantly higher levels of PD-L1 expression following exposure to recombinant GM-CSF or MC38CEA cells (Fig. 4c, d).

## L-MDSC suppress CAR-T through STAT3-dependent PD-L1 expression

To determine whether CAR-T proliferation could be rescued by blocking PD-1/PD-L1 interactions, L-MDSC and

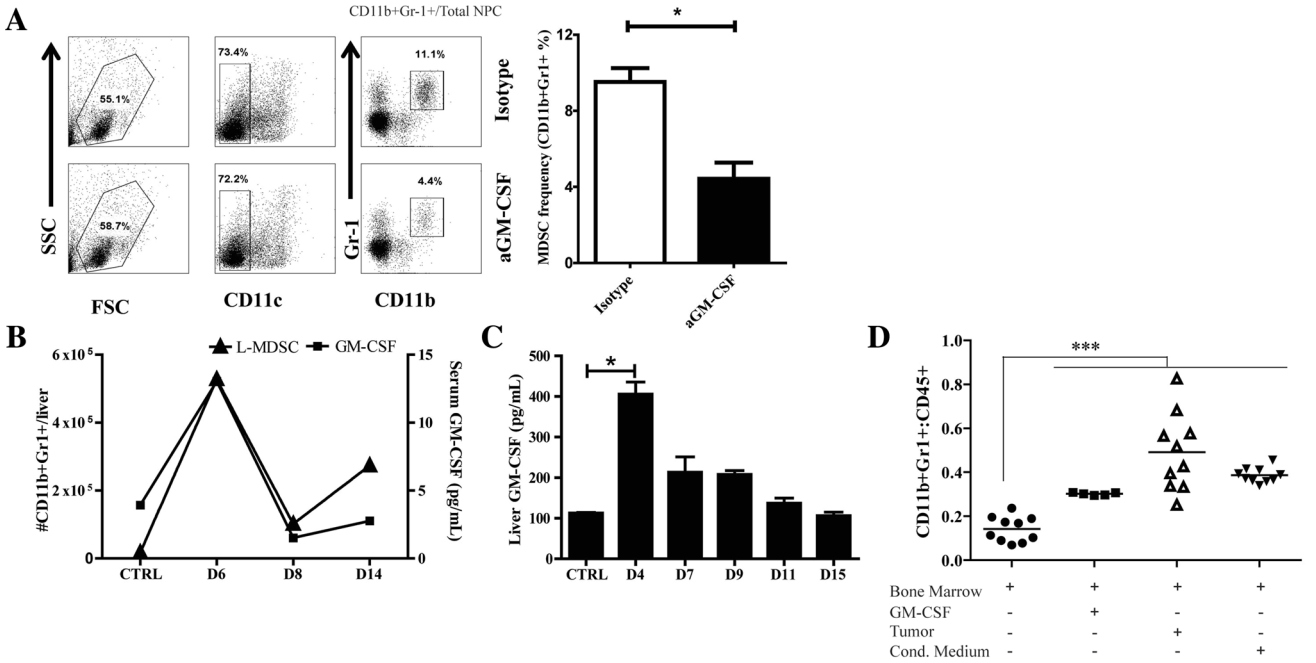


**Fig. 3** L-MDSC expansion is driven by tumor-associated GM-CSF. LM were established by splenic injections of MC38CEA cells, and isotype control (IgG) or anti-GM-CSF antibody (aGM-CSF) was injected intraperitoneally on days 4, 6, and 8 post-tumor establishment. **a** Flow cytometry was used following harvest after 9 days to evaluate MDSC frequency (live, CD11b+Gr-1+ cells) (*right*, representative of three independent experiments). For this experiment, MDSC percentage values reflect analysis of bulk NPC not subjected to fractionation based on CD45 expression. **b** Serum GM-CSF and L-MDSC absolute numbers as determined by flow cytometry were quantified from mice at various time points post-LM establishment or CTRL (non-tumor bearing). **c** Whole liver lysate GM-CSF was measured from mice following LM establishment or CTRL animals. **d** The percentage of cells acquiring an MDSC phenotype (CD11b+Gr-1+) was determined by flow cytometry from bone marrow cells cultured for 3–4 days with exposure to recombinant GM-CSF, GM-CSF-producing MC38CEA tumor, or tumor-conditioned medium. *Bar graphs* represent mean ± SEM; *dots plots* are representative of ≥3 mice per group and have been confirmed with ≥2 separate experiments (*$p \leq 0.05$, ***$p \leq 0.001$)

stimulated CAR-T were co-cultured with and without anti-PD-L1 antibody. L-MDSC suppression of CAR-T proliferation was reversed by PD-L1-blockade (Fig. 5a). Additionally, pre-treating tumor-bearing animals with anti-PD-L1 or performing the assay with PD-1$^{-/-}$ CAR-T also reversed immunosuppression (Fig. 5b). SSG, a chemical inhibitor of SHP-1 and SHP-2 [26] phosphatases critical to PD-1 function, also demonstrated significant reversal of suppression ($p = 0.01$, data not shown), confirming that L-MDSC exploit the PD-1/PD-L1 axis to suppress anti-CEA CAR-T.

We then delved deeper into the mechanism through which L-MDSC upregulate PD-L1 expression. We demonstrated that L-MDSC express GM-CSFR (data not shown) while others demonstrated that signal transducer and activator of transcription 3 (STAT3) regulates GM-CSFR expression [27]. As STAT3 is also known to regulate also PD-L1, we sought to determine whether this was the case in L-MDSC [28]. In an analysis of whole liver lysate, we found that both total and pSTAT3 levels were increased in tumor bearing as compared to control animals ($p = 0.005$ and $p = 0.02$, data not shown). Western blot analysis on purified L-MDSC from tumor-bearing livers revealed an increase in the active phosphorylated form of STAT3 (pSTAT3) relative to total (TSTAT3) protein (Fig. 5c, d). Treatment of L-MDSC isolated from tumor-bearing livers with JSI-124 or celastrol, both potent STAT3 inhibitors [29], resulted in a significant decrease in PD-L1 expression (Fig. 5e, f).

## Improved anti-CEA CAR-T efficacy is achieved by targeting L-MDSC

Having demonstrated that GM-CSF and PD-L1 promote MDSC suppression of CAR-T, we tested GM-CSF and PD-L1 blockade in vivo. Tumor-bearing animals were treated with two doses of regional CAR-T, 3 and 7 days following LM establishment, and received anti-Gr-1, anti-GM-CSF, anti-PD-L1, or the combination of anti-GM-CSF and anti-PD-L1. All mice received IL2 (Fig. 6a). Initially, all animals had similar LM burdens. Bioluminescent imaging demonstrated a delay in tumor progression in mice receiving CAR-T with and without antibody treatments (Fig. 6b–d). Anti-tumor efficacy of anti-CEA CAR-T was improved when used in combination with antibodies that

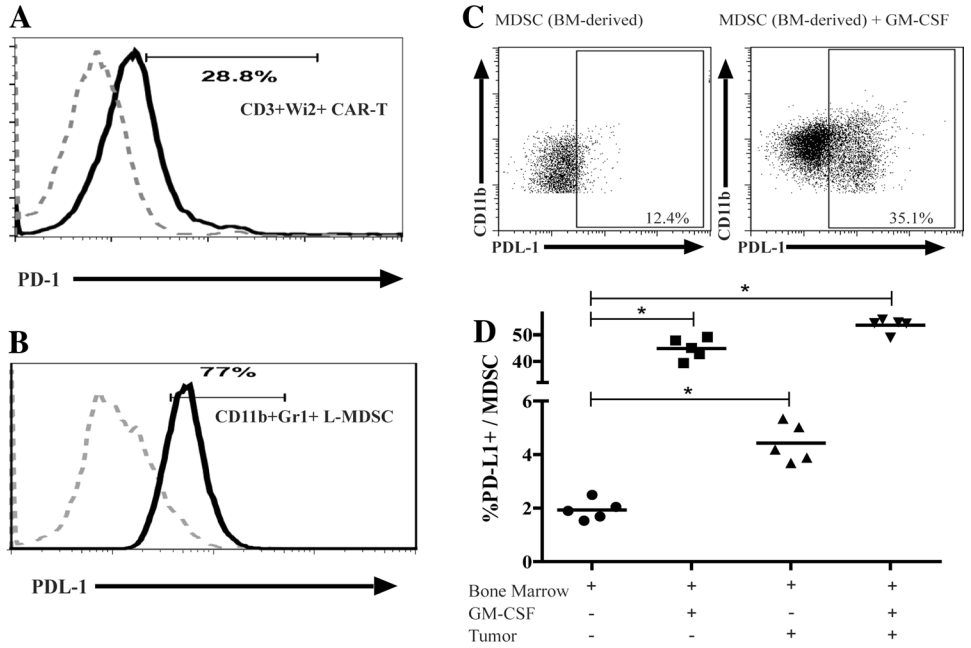


**Fig. 4** L-MDSC suppression through PD-1/PD-L1 is modulated by GM-CSF. **a** Flow cytometry was used to determine PD-1 expression on fresh CAR-T (CAR-T gated as CD3+Wi2+ cells) relative to FMO controls. **b** Flow cytometry was used to determine PD-L1 expression on L-MDSC (gated CD11c−CD11b+Gr-1+) isolated from tumor-bearing mice after 2 weeks of tumor growth relative to FMO controls. **c** Representative *dot plots* indicating PD-L1 expression as determined from BM-derived MDSC (gated as live, CD45+CD11c−CD11b+Gr-1+ cells) following exposure to recombinant GM-CSF or GM-CSF-producing tumor ex vivo. **d** Pooled results from two independent experiments are graphed. *Bar graphs* represent mean ± SEM; *dot plots* and *histograms* are representative of ≥3 mice per group and have been confirmed with ≥2 separate experiments (*$p \leq 0.05$)

suppressed MDSC (Fig. 6b, d). Bioluminescence results indicated a trend toward a reduction in tumor burden with anti-Gr-1, anti-GM-CSF, and anti-PD-L1 treatments (Fig. 6b–d). Survival of the animals in the same groups showed a statistically significant increase in survival of mice treated with CAR-T+anti-GM-CSF compared to CAR-T alone ($p = 0.03$, Fig. 6e).

## Discussion

CAR-T infusions are a promising therapy for solid tumors, but their role in treating LM has yet to be fully explored. Our findings suggest that regional infusion of CAR-T in mice with LM can delay tumor progression, but immunosuppression mediated by L-MDSC in the intrahepatic space prevents complete tumor clearance. GM-CSF drove L-MDSC expansion in response to LM and worked in concert with STAT3 to increase MDSC PD-L1 expression. Expanded PD-L1+ L-MDSC demonstrated potent suppression of CAR-T proliferation. However, MDSC depletion or blockade of MDSC expansion enhanced CAR-T LM cell killing in vivo. Our data provide preclinical rationale for using regional CAR-T infusions in conjunction with agents targeting MDSC immunoinhibitory pathways to treat LM.

Consistent with prior reports, L-MDSC populations dramatically expanded in response to LM [30, 31]. We are the first group, to our knowledge, to demonstrate that anti-CEA CAR-T are suppressed by L-MDSC. Other groups have shown that MDSC induce T cell exhaustion through the PD-1/PD-L1 axis [32] as well as metabolism of L-arginine [33] and nitric oxide (NO) production [34]. A previous report suggested that second-generation CAR-T, which contains the CD28 co-stimulatory moiety, resist suppression by Treg [35]. We demonstrated that CAR-T equipped with the CD28 moiety were in fact vulnerable to suppression by L-MDSC. Accordingly, MDSC depletion improved anti-tumor efficacy of CAR-T in animals with LM. Unfortunately, human MDSC, which can be classified as lin$^-$CD33+CD34+CD15+, or CD11b+CD14+HLA-DR$^-$ [36], cannot presently be similarly targeted with a single antibody. As such, we identified alternative targets for blocking L-MDSC expansion and suppressive function in the setting of LM.

Consistent with our findings, GM-CSF has been previously identified as a mediator of MDSC expansion in other experimental systems [18, 37–40]. The importance of GM-CSF in driving L-MDSC expansion is consistent with findings in pancreas cancer models [38, 40]. Bronte demonstrated increased metastases through MDSC recruitment

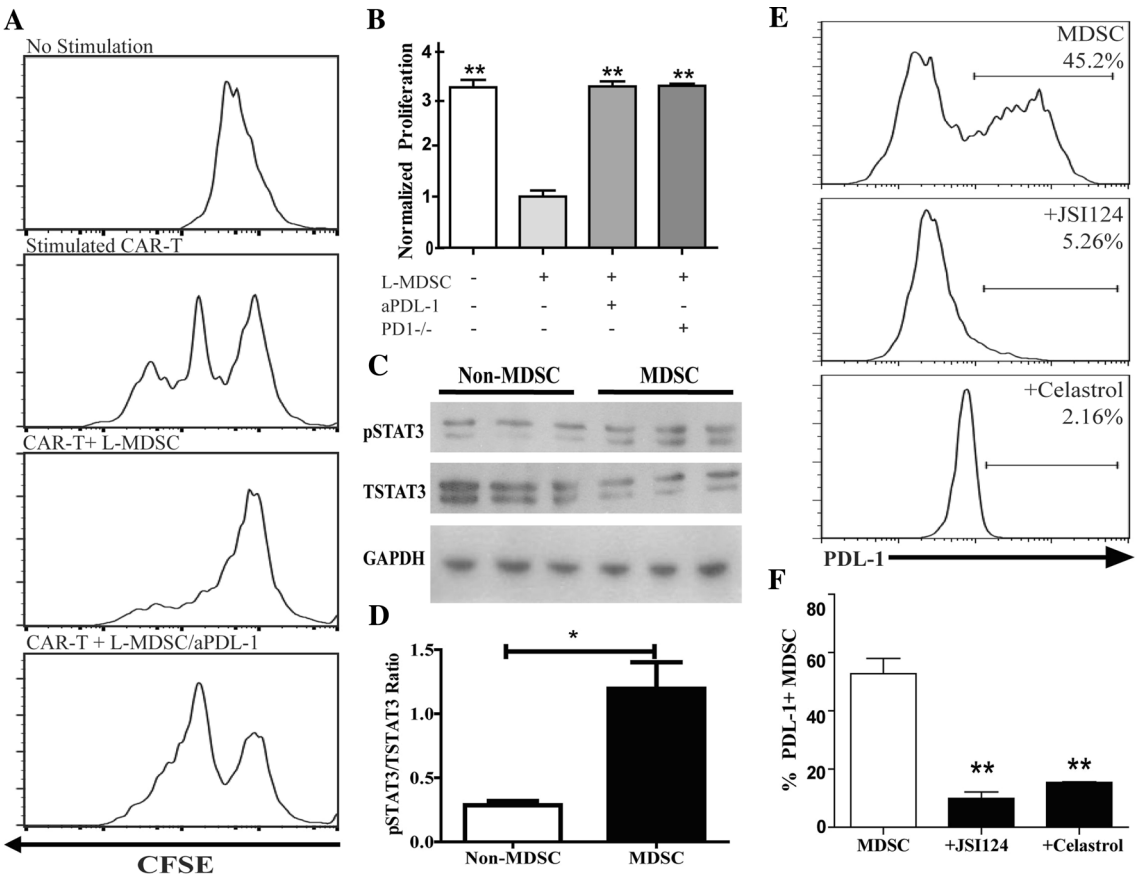


**Fig. 5** L-MDSC suppress CAR-T through STAT3-dependent PD-L1 expression. **a** Representative CFSE histograms that demonstrate CAR-T proliferation (*second panel*) were suppressed by L-MDSC (*third panel*) and rescued by the addition of anti-PD-L1 antibody (aPD-L1). **b** Pooled results from three independent experiments are graphed, with proliferation normalized to that of the minimal proliferation value. The percentage of proliferating CAR-T was calculated based upon CFSE-low cells. **c** Phosphorylated STAT3 (pSTAT3) and total STAT3 (TSTAT3) expression levels in MDSC (CD11b+NPC) and non-MDSC (CD11b-fraction) from tumor-bearing livers were assayed by Western blot. **d** pSTAT3 to TSTAT3 ratio obtained from the Western blot analysis was calculated for MDSC and non-MDSC. **e** Flow cytometry was used to determine PD-L1 expression on L-MDSC following ex vivo culture with the STAT3 inhibitors JSI-124 and celastrol. **f** Pooled results from four independent experiments are graphed. *Bar graphs* represent mean ± SEM; *dot plots* and *histograms* are representative of ≥3 mice per group and have been confirmed with ≥3 separate experiments. Normalized proliferation = experimental %proliferation/%proliferation of CAR-T+MDSC (**$p \leq 0.01$, ***$p \leq 0.001$)

[24], and Dolcetti found GM-CSF necessary for MDSC expansion and tumor tolerance [41]. Likewise, Bayne identified GM-CSF as a necessary driver of CD11b+Gr-1+ cell accumulation in a model of pancreas adenocarcinoma [38]. The intrahepatic space presents a challenging immunosuppressive milieu due to the presence of large number of suppressive cell types other than MDSC, and our findings provide insight into how liver immune cells may suppress effectiveness of CAR-T [16, 42]. While GM-CSF has been used as an adjuvant to promote anti-tumor immunity [43, 44], GM-CSF drives MDSC suppressive function in the liver and other settings [18, 45]. Caution is therefore warranted in applying GM-CSF within immunotherapy protocols. In our model, liver GM-CSF levels peaked 3 days prior to the L-MDSC frequency peak. We speculate that the rapidly expanding L-MDSC population consumed GM-CSF as LM progressed, accounting for the drop in liver and serum GM-CSF levels after 1 week. While we confirmed MC38CEA tumor cells produced GM-CSF, macrophages, T cells, endothelial cells, and fibroblasts normally secrete GM-CSF as well. Although we cannot discount the contribution of GM-CSF production by non-tumor cells in our model, we demonstrated significantly higher levels GM-CSF production by tumor cells as compared to NPC. Tumor-derived GM-CSF promotes tumor progression and failure of immunity [23, 46].

In our model, GM-CSF supported L-MDSC expansion and L-MDSC PD-L1 expression. GM-CSF cooperated with STAT3 in promoting L-MDSC PD-L1 expression. The PD-1/PD-L1 axis is rapidly emerging as a clinically important immunoinhibitory pathway. Previous reports have indicated increased levels of PD-L1 on murine dendritic cells

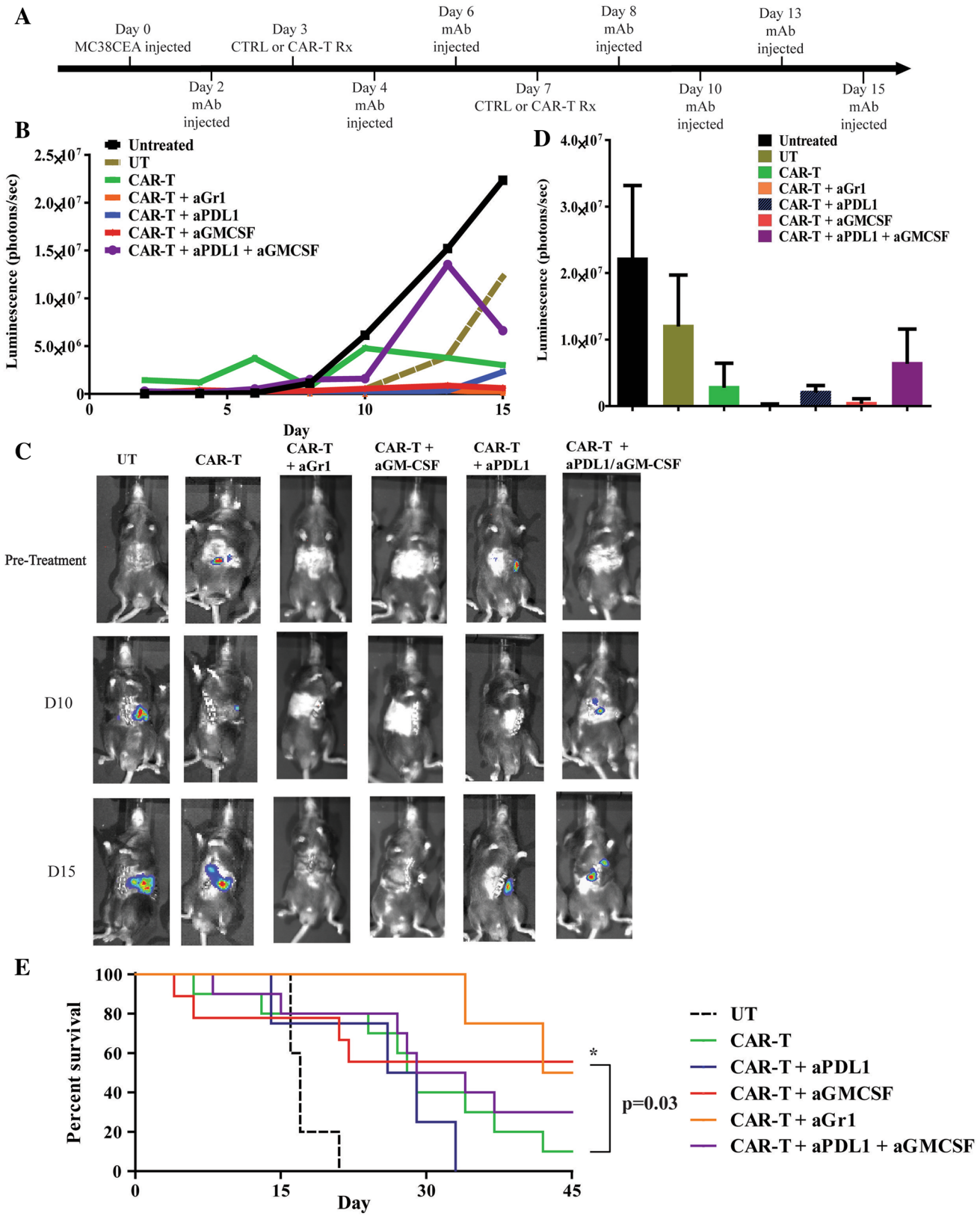
A
Day 0
MC38CEA injected
Day 2
mAb
injected
Day 3
CTRL or CAR-T Rx
Day 4
mAb
injected
Day 6
mAb
injected
Day 7
CTRL or CAR-T Rx
Day 8
mAb
injected
Day 10
mAb
injected
Day 13
mAb
injected
Day 15
mAb
injected
B
Luminescence (photons/sec)
Untreated
UT
CAR-T
CAR-T + aGr1
CAR-T + aPDL1
CAR-T + aGMCSF
CAR-T + aPDL1 + aGMCSF
Day
D
Luminescence (photons/sec)
C
UT
CAR-T
CAR-T + aGr1
CAR-T + aGM-CSF
CAR-T + aPDL1
CAR-T + aPDL1/aGM-CSF
Pre-Treatment
D10
D15
E
Percent survival
Day
p=0.03
UT
CAR-T
CAR-T + aPDL1
CAR-T + aGMCSF
CAR-T + aGr1
CAR-T + aPDL1 + aGMCSF

◀ **Fig. 6** Neutralization of GM-CSF and PD-L1 improves regional anti-CEA CAR-T efficacy. **a** Mice were injected with luciferase-expressing MC38CEA cells to establish LM and received treatments as indicated in addition to daily systemic IL2 support. **b** Mice were injected with luciferin and imaged for 15 days to evaluate tumor progression expressed as bioluminescence (photon/s). **c** Representative images of tumor burden at indicated time points. **d** *Bar graphs* indicate quantified tumor bioluminescence presented at day 15 following LM establishment. Groups were untreated ($n = 3$), untransduced (UT, $n = 5$), CAR-T ($n = 11$), CAR-T+aGr-1 ($n = 10$), CAR-T+aPD-L1 ($n = 5$), CAR-T+aGM-CSF ($n = 10$), CAR-T+aPD-L1+aGM-CSF ($n = 11$). **e** Survival of the animals treated with antibodies was tracked for up to 45 days after tumor injections. Kaplan–Meier curves were constructed and groups compared with the log-rank test. CAR-T+anti-GM-CSF treatment was significantly higher than CAR-T alone ($^*p = 0.03$)

and macrophages [47] after exposure to GM-CSF [48]; however, the effect on MDSC is not well documented. Our finding that both GM-CSF and STAT3 promoted PD-L1 expression on L-MDSC provides rationale for targeting GM-CSF and STAT3 to reverse MDSC suppression of CAR-T. While we did not establish a direct link between GM-CSF and STAT3 in our model, a prior report indicated that GM-CSF receptor activation triggers STAT3 signaling [49] among myeloid cells [28]. Additionally, IL6 signaling may promote STAT3-driven PD-L1 expression by L-MDSC, and further work is required to explore this relationship.

We confirmed the importance of the PD-1/PD-L1 axis [26] for L-MDSC suppression of CAR-T by demonstrating in vitro that L-MDSC were unable to limit proliferation of anti-CEA CAR-T created from knockout mice lacking PD-1. Moreover, CAR-T proliferation in the presence of L-MDSC was also rescued by SHP-1 and SHP-2 inhibition, which prevents PD-1 signaling within CAR-T [50]. L-MDSC may circumvent the effects of PD-L1 blockade by exploiting alternative suppressive pathways, such as indolamine 2, 3-dioxygenase (IDO) [51], arginase, or inducible NO synthase (iNOS) [34], and further studies would be needed to determine whether in vivo IDO or iNOS inhibition affects CAR-T efficacy for LM.

Though CEA+ LM is the primary focus of this report, regional CAR-T infusions are applicable to other malignancies associated with LM. Our work treating LM with CAR-T in combination with anti-Gr-1, anti-GM-CSF or anti-PD-L1 antibodies speaks to the potential clinical merit of neutralizing L-MDSC in order to allow for optimal anti-tumor efficacy. CAR-T in combination with anti-GM-CSF significantly enhanced survival of animals with LM. The surprising observation that a combination of anti-GM-CSF and anti-PD-L1 antibodies did not enhance anti-tumor CAR-T efficacy compared to anti-GM-CSF and anti-PD-L1 alone may be due to the pleiotropic actions of GM-CSF and PD-L1, in addition to an unexpected pro-inflammatory role of PD-L1 in some mouse models [52]. Specifically, the nonsignificant trend toward increased tumor burden in mice treated with both antibodies may be ascribed to the suppression of pro-inflammatory myeloid cells, such as neutrophils or myeloid dendritic cells (mDC), which may inhibit LM progression. Both neutrophils and mDC are partially reliant on GM-CSF and express PD-L1. A combination of antibodies that block both molecules may adversely affect the anti-tumor activity of these cells. The data point to a complex and opposing role of PD-L1 that needs further elucidation. Additional limitations of the present study should be considered. Our work did not specifically address L-MDSC subtypes, which likely exert variable suppressive influence over CAR-T. We were able to demonstrate anti-tumor activity with up to two portal vein CAR-T treatments; however, full remission was not achieved. Multiple regional CAR-T infusions, as done in our phase I study, are likely to be necessary clinically, in the absence of preconditioning, to achieve optimal tumor killing [53].

L-MDSC expand in response to LM and likely exploit multiple, redundant immunosuppressive pathways to prevent tumor eradication by CAR-T. A multifaceted approach will likely be required to achieve the desired level of CAR-T anti-tumor activity in the setting of LM. Identification of STAT3, GM-CSF, and PD-L1 as key mediators of MDSC suppressive function provides strong rationale for targeting these molecules in combination with regional CAR-T infusions for LM.

**Acknowledgments** The authors would like to thank Erica Santos for her technical assistance, Dr. Jeffrey Schlom for providing MC38 and MC38CEA cell lines, Dr. Tasuku Honjo for providing the PD-$1^{-/-}$ mice to begin our in-house breeding, and Dr. Hansen for generously providing the Wi2 anti-idiotype CAR antibody. We would like to thank Dr. John Morgan and Roger Williams Medical Center Core Facility for providing us with the necessary equipment to carry out flow cytometry and in vivo bioluminescence experiments. Support for this work was provided by the National Institutes of Health (1K08CA160662-01A1), the Society of Surgical Oncology Clinical Investigator Award supported by an education grant from Genentech, and the Rhode Island Foundation.

**Conflict of interest** The authors have no conflict of interest to disclose.

## References

1. Donadon M, Ribero D, Morris-Stiff G, Abdalla EK, Vauthey JN (2007) New paradigm in the management of liver-only metastases from colorectal cancer. Gastrointest Cancer Res 1(1):20–27
2. Tomlinson JS, Jarnagin WR, DeMatteo RP, Fong Y, Kornprat P, Gonen M, Kemeny N, Brennan MF, Blumgart LH, D'Angelica M (2007) Actual 10-year survival after resection of colorectal liver metastases defines cure. J Clin Oncol 25(29):4575–4580. doi:10.1200/JCO.2007.11.0833
3. Grothey A, Sargent D (2005) Overall survival of patients with advanced colorectal cancer correlates with availability of fluorouracil, irinotecan, and oxaliplatin regardless of whether doublet or single-agent therapy is used first line. J Clin Oncol 23(36):9441–9442. doi:10.1200/JCO.2005.04.4792

4. Rothenberg ML, Oza AM, Bigelow RH, Berlin JD, Marshall JL, Ramanathan RK, Hart LL, Gupta S, Garay CA, Burger BG, Le Bail N, Haller DG (2003) Superiority of oxaliplatin and fluorouracil-leucovorin compared with either therapy alone in patients with progressive colorectal cancer after irinotecan and fluorouracil-leucovorin: interim results of a phase III trial. J Clin Oncol 21(11):2059–2069. doi:10.1200/JCO.2003.11.126
5. Katz SC, Pillarisetty V, Bamboat ZM, Shia J, Hedvat C, Gonen M, Jarnagin W, Fong Y, Blumgart L, D'Angelica M, DeMatteo RP (2009) T cell infiltrate predicts long-term survival following resection of colorectal cancer liver metastases. Ann Surg Oncol 16(9):2524–2530. doi:10.1245/s10434-009-0585-3
6. Katz SC, Bamboat ZM, Maker AV, Shia J, Pillarisetty VG, Yopp AC, Hedvat CV, Gonen M, Jarnagin WR, Fong Y, D'Angelica MI, DeMatteo RP (2013) Regulatory T cell infiltration predicts outcome following resection of colorectal cancer liver metastases. Ann Surg Oncol 20(3):946–955. doi:10.1245/s10434-012-2668-9
7. Hodi FS, O'Day SJ, McDermott DF, Weber RW, Sosman JA, Haanen JB, Gonzalez R, Robert C, Schadendorf D, Hassel JC, Akerley W, van den Eertwegh AJ, Lutzky J, Lorigan P, Vaubel JM, Linette GP, Hogg D, Ottensmeier CH, Lebbé C, Peschel C, Quirt I, Clark JI, Wolchok JD, Weber JS, Tian J, Yellin MJ, Nichol GM, Hoos A, Urba WJ (2010) Improved survival with ipilimumab in patients with metastatic melanoma. N Engl J Med 363(8):711–23. doi: 10.1056/NEJMoa1003466
8. Kantoff PW, Higano CS, Shore ND, Berger ER, Small EJ, Penson DF, Redfern CH, Ferrari AC, Dreicer R, Sims RB, Xu Y, Frohlich MW, Schellhammer PF, IMPACT Study Investigators (2010) Sipuleucel-T immunotherapy for castration-resistant prostate cancer. N Engl J Med 363(5):411–22. doi: 10.1056/NEJMoa1001294
9. Davila ML, Kloss CC, Gunset G, Sadelain M (2013) CD19 CAR-targeted T cells induce long-term remission and B cell Aplasia in an immunocompetent mouse model of B cell acute lymphoblastic leukemia. PLoS One 8(4):e61338. doi:10.1371/journal.pone.0061338
10. Grupp SA, Kalos M, Barrett D, Aplenc R, Porter DL, Rheingold SR, Teachey DT, Chew A, Hauck B, Wright JF, Milone MC, Levine BL, June CH (2013) Chimeric antigen receptor-modified T cells for acute lymphoid leukemia. N Engl J Med 368(16):1509–1518. doi:10.1056/NEJMoa1215134
11. Lo AS, Ma Q, Liu DL, Junghans RP (2010) Anti-GD3 chimeric sFv-CD28/T-cell receptor zeta designer T cells for treatment of metastatic melanoma and other neuroectodermal tumors. Clin Cancer Res 16(10):2769–2780. doi:10.1158/1078-0432.CCR-10-0043
12. Midiri G, Amanti C, Benedetti M, Campisi C, Santeusanio G, Castagna G, Peronace L, Di Tondo U, Di Paola M, Pascal RR (1985) CEA tissue staining in colorectal cancer patients. A way to improve the usefulness of serial serum CEA evaluation. Cancer 55(11):2624–2629
13. Emtage PC, Lo AS, Gomes EM, Liu DL, Gonzalo-Daganzo RM, Junghans RP (2008) Second-generation anti-carcinoembryonic antigen designer T cells resist activation-induced cell death, proliferate on tumor contact, secrete cytokines, and exhibit superior antitumor activity in vivo: a preclinical evaluation. Clin Cancer Res 14(24):8112–8122. doi:10.1158/1078-0432.CCR-07-4910
14. Saied A, Licata L, Burga RA, Thorn M, McCormack E, Stainken BF, Assanah EO, Khare PD, Davies R, Espat NJ, Junghans RP, Katz SC (2014) Neutrophil:lymphocyte ratios and serum cytokine changes after hepatic artery chimeric antigen receptor-modified T-cell infusions for liver metastases. Cancer Gene Ther 21(11):457–462. doi:10.1038/cgt.2014.50
15. Almand B, Clark JI, Nikitina E, van Beynen J, English NR, Knight SC, Carbone DP, Gabrilovich DI (2001) Increased production of immature myeloid cells in cancer patients: a mechanism of immunosuppression in cancer. J Immunol 166(1):678–689
16. Katz SC, Pillarisetty VG, Bleier JI, Kingham TP, Chaudhry UI, Shah AB, DeMatteo RP (2005) Conventional liver CD4 T cells are functionally distinct and suppressed by environmental factors. Hepatology 42(2):293–300. doi:10.1002/hep.20795
17. Hochst B, Schildberg FA, Sauerborn P, Gabel YA, Gevensleben H, Goltz D, Heukamp LC, Turler A, Ballmaier M, Gieseke F, Muller I, Kalff J, Kurts C, Knolle PA, Diehl L (2013) Activated human hepatic stellate cells induce myeloid derived suppressor cells from peripheral blood monocytes in a CD44-dependent fashion. J Hepatol 59(3):528–535. doi:10.1016/j.jhep.2013.04.033
18. Serafini P, Borrello I, Bronte V (2006) Myeloid suppressor cells in cancer: recruitment, phenotype, properties, and mechanisms of immune suppression. Semin Cancer Biol 16(1):53–65. doi:10.1016/j.semcancer.2005.07.005
19. Diaz-Montero CM, Salem ML, Nishimura MI, Garrett-Mayer E, Cole DJ, Montero AJ (2009) Increased circulating myeloid-derived suppressor cells correlate with clinical cancer stage, metastatic tumor burden, and doxorubicin-cyclophosphamide chemotherapy. Cancer Immunol Immunother 58(1):49–59. doi:10.1007/s00262-008-0523-4
20. Abate-Daga D, Hanada K, Davis JL, Yang JC, Rosenberg SA, Morgan RA (2013) Expression profiling of TCR-engineered T cells demonstrates overexpression of multiple inhibitory receptors in persisting lymphocytes. Blood 122(8):1399–1410. doi:10.1182/blood-2013-04-495531
21. Sharpe AH, Wherry WJ, Ahmed R, Freeman GJ (2007) The function of programmed cell death 1 and its ligands in regulating autoimmunity and infection. Nat Immunol 8(3):239–245
22. Ghosh CC, Mukherjee A, David S, Knaus UG, Stearns-Kurosawa DJ, Kurosawa S, Parikh SM (2012) Impaired function of the Tie-2 receptor contributes to vascular leakage and lethality in anthrax. Proc Natl Acad Sci USA 109(25):10024–10029. doi:10.1073/pnas.1120755109
23. Lesokhin AM, Hohl TM, Kitano S, Cortez C, Hirschhorn-Cymerman D, Avogadri F, Rizzuto GA, Lazarus JJ, Pamer EG, Houghton AN, Merghoub T, Wolchok JD (2012) Monocytic CCR2(+) myeloid-derived suppressor cells promote immune escape by limiting activated CD8 T-cell infiltration into the tumor microenvironment. Cancer Res 72(4):876–886. doi:10.1158/0008-5472.CAN-11-1792
24. Bronte V, Chappell DB, Apolloni E, Cabrelle A, Wang M, Hwu P, Restifo NP (1999) Unopposed production of granulocyte–macrophage colony-stimulating factor by tumors inhibits CD8+ T cell responses by dysregulating antigen-presenting cell maturation. J Immunol 162(10):5728–5737
25. Schmidt K, Zilio S, Schmollinger JC, Bronte V, Blankenstein T, Willimsky G (2013) Differently immunogenic cancers in mice induce immature myeloid cells that suppress CTL in vitro but not in vivo following transfer. Blood 121(10):1740–1748. doi:10.1182/blood-2012-06-436568
26. John LB, Devaud C, Duong CM, Yong C, Beavis PA, Haynes NM, Chow MT, Smyth MJ, Kershaw MH, Darcy PK (2013) Anti-PD-1 antibody therapy potently enhances the eradication of established tumors by gene-modified T cells. Clin Cancer Res 19(20):5636–5646. doi:10.1158/1078-0432.CCR-13-0458
27. Li P, Harris D, Liu Z, Rozovski U, Ferrajoli A, Wang Y, Bueso-Ramos C, Hazan-Halevy I, Grgurevic S, Wierda W, Burger J, O'Brien S, Faderl S, Keating M, Estrov Z (2014) STAT3-activated GM-CSFRalpha translocates to the nucleus and protects CLL cells from apoptosis. Mol Cancer Res 12(9):1267–1282. doi:10.1158/1541-7786.MCR-13-0652-T

28. Wolfle SJ, Strebovsky J, Bartz H, Sahr A, Arnold C, Kaiser C, Dalpke AH, Heeg K (2011) PD-L1 expression on tolerogenic APCs is controlled by STAT-3. Eur J Immunol 41(2):413–424. doi:10.1002/eji.201040979
29. Nefedova Y, Nagaraj S, Rosenbauer A, Muro-Cacho C, Sebti SM, Gabrilovich DI (2005) Regulation of dendritic cell differentiation and antitumor immune response in cancer by pharmacologic-selective inhibition of the janus-activated kinase 2/signal transducers and activators of transcription 3 pathway. Cancer Res 65(20):9525–9535. doi:10.1158/0008-5472.CAN-05-0529
30. Ilkovitch DLD (2009) The liver is a site for tumor-induced myeloid-derived suppressor cell accumulation and immunosuppression. Cancer Res 69(13):5514–5521
31. Zhao L, Lim SY, Gordon-Weeks AN, Tapmeier TT, Im JH, Cao Y, Beech J, Allen D, Smart S, Muschel RJ (2013) Recruitment of a myeloid cell subset (CD11b/Gr1 mid) via CCL2/CCR2 promotes the development of colorectal cancer liver metastasis. Hepatology 57(2):829–839. doi:10.1002/hep.26094
32. Blank C, Mackensen A (2007) Contribution of the PD-L1/PD-1 pathway to T-cell exhaustion: an update on implications for chronic infections and tumor evasion. Cancer Immunol Immunother 56(5):739–745. doi:10.1007/s00262-006-0272-1
33. Bronte V, Serafini P, Mazzoni A, Segal DM, Zanovello P (2003) L-arginine metabolism in myeloid cells controls T-lymphocyte functions. Trends Immunol 24(6):302–306
34. Mazzoni A, Bronte V, Visintin A, Spitzer JH, Apolloni E, Serafini P, Zanovello P, Segal DM (2002) Myeloid suppressor lines inhibit T cell responses by an NO-dependent mechanism. J Immunol 168(2):689–695
35. Loskog A, Giandomenico V, Rossig C, Pule M, Dotti G, Brenner MK (2006) Addition of the CD28 signaling domain to chimeric T-cell receptors enhances chimeric T-cell resistance to T regulatory cells. Leukemia 20(10):1819–1828. doi:10.1038/sj.leu.2404366
36. Greten TF, Manns MP, Korangy F (2011) Myeloid derived suppressor cells in human diseases. Int Immunopharmacol 11(7):802–807. doi:10.1016/j.intimp.2011.01.003
37. Gabrilovich DI, Nagaraj S (2009) Myeloid-derived suppressor cells as regulators of the immune system. Nat Rev Immunol 9(3):162–174. doi:10.1038/nri2506
38. Bayne LJ, Beatty GL, Jhala N, Clark CE, Rhim AD, Stanger BZ, Vonderheide RH (2012) Tumor-derived granulocyte–macrophage colony-stimulating factor regulates myeloid inflammation and T cell immunity in pancreatic cancer. Cancer Cell 21(6):822–835. doi:10.1016/j.ccr.2012.04.025
39. Kohanbash G, McKaveney K, Sakaki M, Ueda R, Mintz AH, Amankulor N, Fujita M, Ohlfest JR, Okada H (2013) GM-CSF promotes the immunosuppressive activity of glioma-infiltrating myeloid cells through interleukin-4 receptor-alpha. Cancer Res 73(21):6413–6423. doi:10.1158/0008-5472.CAN-12-4124
40. Pylayeva-Gupta Y, Lee KE, Hajdu CH, Miller G, Bar-Sagi D (2012) Oncogenic Kras-induced GM-CSF production promotes the development of pancreatic neoplasia. Cancer Cell 21(6):836–847. doi:10.1016/j.ccr.2012.04.024
41. Dolcetti L, Peranzoni E, Ugel S, Marigo I, Fernandez Gomez A, Mesa C, Geilich M, Winkels G, Traggiai E, Casati A, Grassi F, Bronte V (2010) Hierarchy of immunosuppressive strength among myeloid-derived suppressor cell subsets is determined by GM-CSF. Eur J Immunol 40(1):22–35. doi:10.1002/eji.200939903
42. Katz SC, Pillarisetty VG, Bleier JI, Shah AB, DeMatteo RP (2004) Liver sinusoidal endothelial cells are insufficient to activate T cells. J Immunol 173(1):230–235
43. Dranoff G, Jaffee E, Lazenby A, Golumbek P, Levitsky H, Brose K, Jackson V, Hamada H, Pardoll D, Mulligan RC (1993) Vaccination with irradiated tumor cells engineered to secrete murine granulocyte–macrophage colony-stimulating factor stimulates potent, specific, and long-lasting anti-tumor immunity. Proc Natl Acad Sci USA 90(8):3539–3543
44. Nemunaitis J (2003) GVAX (GMCSF gene modified tumor vaccine) in advanced stage non small cell lung cancer. J Control Release 91(1–2):225–231
45. Young MR, Wright MA, Lozano Y, Prechel MM, Benefield J, Leonetti JP, Collins SL, Petruzzelli GJ (1997) Increased recurrence and metastasis in patients whose primary head and neck squamous cell carcinomas secreted granulocyte–macrophage colony-stimulating factor and contained CD34+ natural suppressor cells. Int J Cancer 74(1):69–74
46. Serafini P, Carbley R, Noonan KA, Tan G, Bronte V, Borrello I (2004) High-dose granulocyte–macrophage colony-stimulating factor-producing vaccines impair the immune response through the recruitment of myeloid suppressor cells. Cancer Res 64(17):6337–6343. doi:10.1158/0008-5472.CAN-04-0757
47. Yamazaki T, Akiba H, Iwai H, Matsuda H, Aoki M, Tanno Y, Shin T, Tsuchiya H, Pardoll DM, Okumura K, Azuma M, Yagita H (2002) Expression of programmed death 1 ligands by murine T cells and APC. J Immunol 169(10):5538–5545
48. Gaudreau S, Guindi C, Menard M, Benabdallah A, Dupuis G, Amrani A (2010) GM-CSF induces bone marrow precursors of NOD mice to skew into tolerogenic dendritic cells that protect against diabetes. Cell Immunol 265(1):31–36. doi:10.1016/j.cellimm.2010.06.010
49. Valdembri D, Serini G, Vacca A, Ribatti D, Bussolino F (2002) In vivo activation of JAK2/STAT-3 pathway during angiogenesis induced by GM-CSF. FASEB J 16(2):225–227. doi:10.1096/fj.01-0633fje
50. Mauldin IS, Tung KS, Lorenz UM (2012) The tyrosine phosphatase SHP-1 dampens murine Th17 development. Blood 119(19):4419–4429. doi:10.1182/blood-2011-09-377069
51. Yu J, Du W, Yan F, Wang Y, Li H, Cao S, Yu W, Shen C, Liu J, Ren X (2013) Myeloid-derived suppressor cells suppress antitumor immune responses through IDO expression and correlate with lymph node metastasis in patients with breast cancer. J Immunol 190(7):3783–3797. doi:10.4049/jimmunol.1201449
52. Bodhankar S, Chen Y, Vandenbark AA, Murphy SJ, Offner H (2013) PD-L1 enhances CNS inflammation and infarct volume following experimental stroke in mice in opposition to PD-1. J Neuroinflammation 10:111. doi:10.1186/1742-2094-10-111
53. Katz SC, Burga R, Wang L, Mooring W, Davies R, Stainken BF, Assanah EO, Khare P, Ma Q, Espat NJ, Junghans RP (2014) Hepatic Immunotherapy for Metastases (HITM): a phase I trial of anti-CEA genetically modified T cells for unresectable adenocarcinoma. Society of Surgical Oncology 67th Annual Cancer Symposium, Phoenix, AZ